

EPICENTRAL LOCATION OF REGIONAL SEISMIC EVENTS BASED ON EMPIRICAL GREEN FUNCTIONS FROM AMBIENT NOISE

Michael H. Ritzwoller, Mikhail P. Barmin, Anatoli L. Levshin, and Yingjie Yang

University of Colorado at Boulder

Sponsored by the National Nuclear Security Administration

Award No. DE-AC52-09NA29326

Proposal No. BAA09-50

ABSTRACT

The purpose of this research is to develop and test a novel method of regional seismic event location based on exploiting Empirical Green's Functions (EGF) that are produced from ambient noise. Elastic EGFs between pairs of seismic stations are determined by cross-correlating long ambient noise time-series recorded at the two stations. The EGFs principally contain Rayleigh and Love wave energy and our focus is placed on utilizing these signals between 5- and 15-sec periods. By comparing the tabulated EGFs in the frequency-time domain with similarly transformed records of seismic events (earthquakes, explosions, mine collapses) obtained by a network of remote stations, we have tested the method by locating events in the western USA for which other methods provide accurate locations (Californian Ground Truth earthquakes, the mine collapse in Utah). Data from the EarthScope USArray were used primarily. The location errors for GT1 earthquakes in California and the Crandall mine collapse in Utah were on average less than 1 km with origin time errors less than 1 s. These results were described in detail in Ritzwoller et al. (2009). During the past year we continued to refine the method and evaluate its capabilities. The ability of this approach to locate seismic events using a limited number of recording stations with significant open azimuth has been shown. We applied this method to less ideal environments locating small seismic events with magnitude 3.0-3.7 in Utah, with location accuracy better than 0.5 km relative to the University of Utah network locations. The effects of unknown source mechanism and depth on location were studied and are presented here. All research to date is described in detail by Barmin et al. (2010). Future work will continue to refine the location procedure and explore its ability to constrain depth and the moment tensor using ambient noise.

OBJECTIVES

The purpose of this research is to improve seismic event location accuracy and event characterization by exploiting Empirical Green's Functions (EGFs) that emerge by cross-correlating long time sequences of ambient noise observed at pairs of seismic stations. Because ambient noise EGFs are dominated by surface waves, the method uses surface wave energy for location purposes. Present efforts apply Rayleigh wave EGFs from 5 to 15 sec period to the epicentral location problem. The method of epicentral location as well as proof-of-concept applications for a series of seismic events in the western US have been described by Ritzwoller et al. (2009) and more recently and completely by Barmin et al. (2010). During the past year we continued to refine the method, estimated its ability to locate events with smaller magnitudes ($3 < M < 4$), and investigated the intrinsic limitations of the method as a function of number of recording stations and open azimuth. In addition, the effects of unknown source mechanism and depth on location were studied. Future work will continue to refine the location procedure and explore the ability to constrain depth and the moment tensor using ambient noise.

RESEARCH ACCOMPLISHED

1. Methodology

The main features of the epicentral location method based on ambient noise EGFs are as follows:

a) We assume that inside of "the region of interest" where seismic events may occur, a temporary dense local array, termed the **base stations**, is deployed. Second, there is a more distant permanent (but potentially sparse) regional network of stations termed the **remote stations** (Figure 1). Using what are now well established methods (e.g., Bensen et al. (2007), the EGFs from every base to every remote station are computed. At this stage of the project, we use only vertical-to-vertical components of EGFs, which are dominated by Rayleigh waves.

b) The amplitude spectra of EGFs and events recorded at remote stations are normalized without changing the phase spectra. This is done by replacing the amplitude spectrum of the event record with the amplitude spectrum of the EGF, or by replacing both the EGF and event record's amplitude spectrum with the square root of the product of the amplitude spectrum of the event and the EGF.

c) The set of these EGFs is transformed by means of frequency-time analysis (FTAN) as described by Levshin et al. (1971, 1980) into two-dimensional (frequency-time) representations of signal power in a period band and group velocity window corresponding to the fundamental mode of Rayleigh wave in the continental crust. Typically, we select a period range of 5-15 s and a group velocity range of 2.5-4.0 km/s.

d) We cover the "region of interest" by a grid of points whose spacing depends on the density of the base stations array. For each grid point we calculate the so-called **Composite EGFs (CEGFs)** by transforming and stacking the individual EGFs for a given remote station over the base stations. The transformation is done by rescaling the FTAN-diagrams in time according to the distance between a grid point and a remote station. At this stage of the method's development we assume that group velocity in the selected period range does not depend on frequency, and do not use the phase velocity information.

e) The same transformation is applied to the signals recorded by all remote stations. Now for each grid point and each remote station we have an FTAN-diagram of the CGF and the event record. An example of this pair of diagrams is shown in Figure 2a.

f) The next step is cross-correlation in the time domain of the two types of FTAN-diagrams: from event records at all remotes stations and CEGFs for all points of the grid. The time delays of the maximum amplitudes of the cross-correlation functions (Figure 2b) are found and used to construct a quadratic functional of residuals similar to that used in body wave hypocentral location. The grid point with the minimal value of this functional is considered as the epicenter, and the average value of the residuals at this point provides an estimate of the origin time.

g) The confidence ellipse for the position of the epicenter is constructed following the method of Flinn (1965).

2. Location of weaker events in Utah

Ritzwoller et al. (2009) demonstrated the application of the method to GT1 earthquakes in California with $4 < M_b < 5$ and found that average mislocation for these events was about 1 km. To investigate how the method works when applied to events smaller than about magnitude 4.0, we applied it to locate smaller events ($3 < m_b < 4.0$) that occurred in Utah in 2007 and 2008. The location parameters used in this test were: grid size 200 m, $\rho_1=400$ km, $\rho_2=100$ km. These events were well located and characterized by the University of Utah Seismic Stations (UUSS) and by the Department of Earth and Atmospheric Sciences at Saint Louis University (SLU) (J. C. Pechmann, personal communication). Information about these events is given in Table 1. The configuration of stations is shown in Figure 3a and an example of location for one of these earthquakes is given in Figure 3b. Average mislocation is less than 500 m, which indicates the method appears to work well with little modification for events with magnitudes between 3.0 and 4.0. The smaller mislocation for the Utah events compared with the California events may be due to source depth, as these smaller events may be either shallower or deeper than the earthquakes in California. The effect of event depth on mislocation is discussed further in section 3. The location method may be able to be improved further by tuning the band width of the method to the magnitude of the event.

3. Accuracy of location

A number of effects on the accuracy of location are discussed in this section. A more complete discussion is presented by Barmin et al. (2010).

a) **Technical Effects:** There are a number of technical variables that affect the accuracy of locations. We have used EGFs and event seismograms with a time sampling rate of 1 sps, which leads to errors up to 0.5 s in timing of the resulting correlograms. Increasing sampling rates to 10 sps improves the location of well located events but has little effect for events mislocated by 1 km or worse. The size of the spatial grid spacing also affects accuracy, of course.

b) **Observational Network:** The number of remote stations and their geometry relative to the located events are important factors in location accuracy. To evaluate how the number of remote stations and their azimuthal distribution influence location accuracy we focus tests on the TA station S10A in Central Nevada as a virtual earthquake (Figure 4a). Using a jack-knife procedure, we systematically reduced the number of remote stations participating in the location from 126 to 10, while preserving a more or less homogeneous azimuthal coverage. This procedure included 10 runs for each given number of remote stations, but with different ensembles of stations selected. In order to remove the effect of grid increment, we performed locations on a very fine grid (25 m). The average of the mislocations for the 12 runs is shown in Figure 4b as a function of the number of stations, presented with standard deviations. Note that the expected location error is less than 600 m even when the number of remote stations reduces to 10. Mislocation asymptotically approaches about 250 m, for large number of stations and low open azimuth, which we take as the practical limit for the current location algorithm when source mechanism and depth are eliminated. This residual error appears to be determined largely by time discretization (1 sps here).

We have also systematically investigated the effect of open azimuth by eliminating remote stations in azimuthal sectors that vary in size from 30° to 240° . The azimuthal position of each sector of a given size was changed 12 times by shifting the central azimuth of the sector by 30° . The average mislocations for 12 runs as a function of open azimuth plotted with the standard deviations are shown in Figure 4c. As with most location methods, open azimuth is more important than number of remote stations for location accuracy. In particular, as open azimuth grows above about 240° , location accuracy degrades rapidly. As long as open azimuth is less than 240° , however, location errors are expected to be less than 500 m and approach 250 m as open azimuth shrinks.

c) **Event Source Mechanism and Depth:** The most significant physical effects on location accuracy are source mechanism and depth. EGFs determined from ambient noise correspond to surface sources with a predominant source mechanism close to a vertical force. The event seismograms, however, may result from different types of sources at different depths; e.g., earthquakes within Earth's crust, volcanic explosions, meteoritic impacts, explosions, mine collapses, or other human-related excitation processes. The radiation pattern of Rayleigh wave excited by an earthquake is defined by a complex function $E(\omega, h, \mathbf{M})$, which depends on the frequency ω , the source moment tensor \mathbf{M} and depth h as well as local structure, and is quite variable. The function $\arg(E(\omega))$ is the so-called the source phase, and its derivative with ω is the source group time shift. Because the envelopes of event

records and EGFs are what we compare in the frequency-time domain to determine the epicenter, it is group time shift (rather than source phase) that is the relevant effect of event mechanism and depth. Levshin et al. (1999) discuss group time shifts expected for different types of events in detail, and we only summarize briefly here.

- (1) Group time delays are generally much smaller than the source phase delays. This is because the phase delays tend to change relatively slowly with frequency and is one of the reasons we have ignored phase information in the current version of the location method. Nevertheless, group time delays are not negligible and can bias locations.
- (2) Group time shifts are anti-symmetric in epicenter to station azimuth; i.e., changing azimuth by 180° changes only the sign of the delay. Group time shifts differing in azimuth by 180° , therefore, will constructively interfere. Thus, averaging residuals over azimuth while searching for the source position only partially suppresses the effect of group time delays on location.
- (3) For events at the free surface, group time delays are zero for any source mechanism due to the zero amplitude of tangential stress near the free surface. For very shallow depth events (less than 1 km) group time delays will be very small. Thus, shallow events will have small location bias due to source mechanism. This is probably why the Crandall Canyon Mine collapse (see Pechmann et al.(2007)) and small event #3 in Utah (Table 1) were located so well.
- (4) For some mechanisms, such as a pure normal, pure thrust, or a pure strike-slip, group time delays are exactly zero. For pure normal and thrust faults (45° dip and 90° slip) the real part of the expression for the radiation term E is zero. For pure strike-slip faults (90° dip and 0° slip), the imaginary part of E (traction at the surface) is zero. In these cases, $\arg(E)$ and the frequency derivative of $\arg(E)$, which is the group time delay, will be zero. As discussed by Levshin et al. (1999), the source mechanism for most crustal earthquakes is relatively close to these pure mechanisms.

These observations demonstrate that the epicentral location method based on the envelope of ambient noise EGFs will be biased minimally by events that are near the surface or that possess nearly strike-slip, thrust, or normal faulting mechanisms. It remains to be determined numerically how bias sets on as events deepen and mechanisms diverge from these pure types. Numerical simulations of group time delays for events between depths of 2 and 20 km show significant variability with depth, azimuth from the source, and period. Because source mechanisms at these depths typically are close to pure strike-slip, thrust, or normal fault mechanisms, they create very small group time delays (from 0 to 1 s) at periods between 6 and 15 s. More complicated mechanisms, however, can create delays up to (3-4) s, depending on azimuth, depth and period. To quantify group time shifts for a variety of source mechanisms and depths for crustal events we computed simulated Green's functions for a laterally homogeneous model typical of central Nevada (Shapiro and Ritzwoller, 2002) using a surface wave 1-D synthetic code. The base and remote stations used are those shown in Figure 4a. The simulated Green's functions correspond to a vertical force acting at the Earth's surface. We also calculated simulated event seismograms at remote stations for four events with a fixed geographical position within the base network. These events have the source mechanisms shown in the upper part of Figure 5. These mechanisms are similar to pure normal (red) and thrust (green) faults, a vertical thrust fault (navy blue), and a strike-slip fault (light blue), but the corresponding angles characterizing the double couple mechanism (dip and rake) are 15° - 20° different from the pure mechanisms, which is sufficient to produce a significant group time shift. The polar diagrams in Figure 5a show the azimuthal distribution of group time residuals for the corresponding mechanisms with source depths of 2, 5, and 10 km. Note that our location method is based on cross-correlating frequency-time diagrams between 7 and 15 s periods. Thus, the results in Fig. 5a are frequency averaged.

Applying our location technique to the simulated data we find errors in source locations as a function of source depth for the four mechanisms, as seen in Figure 5b. Shallow focus events (depths less than about 1 km) produce very small group time shifts and, therefore, minimal location bias. Similarly, events deeper than about 7 km have location errors smaller than 500 m, at least given the period band of this study (7-15 s). Generally, events with mechanisms similar to thrust or normal faults will have a larger mislocation than those similar to strike-slip. Therefore, non-strike-slip earthquakes with depths between 1 and 5 km provide the greatest challenge for our method.

Our current method is integrated over frequency and it is possible that in the location process the observation of the azimuthal distribution of the group time residuals as a function of period may be used to provide information about the accuracy of the epicentral location or provide information about source depth. Figures 6- 8 present polar diagrams of theoretical group time shifts as a function of period for three event depths for the same

mechanisms as in Figure 5. These results indicate that the azimuthal patterns of group time shifts tend not to change appreciably with period, but the amplitudes can vary strongly. Thus, in the location procedure, the observation of frequency-independent group time residuals is evidence that the epicenter of the event has not been strongly biased by source mechanism. Conversely, the observation of strong frequency-dependence is evidence that the epicenter may be biased, but that the event probably occurred between depths of about 1 and 5 km.

4. Further directions for the method's improvement

Among possible directions for improvement which we plan to investigate during the coming year are:

- (1) The refinement of the EGFs' database by using more detailed time discretization and phase match filtering procedures for improving the signal-to-noise ratio;
- (2) applying frequency-dependent group time transformation of the FTAN-diagram of the EGFs and the event records;
- (3) incorporation of phase information and the transformation of EGFs into Composite EGFs based on tomographic group and phase velocity maps for the region of interest (e.g., Moschetti et al., 2007; Lin et al., 2008);
- (4) the application of information about the frequency-dependence of the residuals to provide information about the source depth and mechanism;
- (5) considering not only vertical but also transverse components of the EGFs which are dominated by Love waves.

Many parameters define the technical instantiation of the method, such as the frequency band, group velocity window, base/remote station geometry, the spatial grid, and the time series sampling rate. These parameters can be varied systematically to tune the method to different observational settings and for events of different magnitude and character.

CONCLUSIONS AND RECOMMENDATIONS

The method to locate the epicenter of regional seismic events based on the envelope of Empirical Green's Functions determined from ambient seismic noise which has been described here and by Barmin et al. (2010) has several features that make it a useful addition to existing location methods.

- Its accuracy does not require knowledge of Earth structure.
- It works for weak events where the detection of body wave phases may be problematic.
- The empirical Green's functions (EGFs) computed during a temporary deployment of a base network (such as the USArray Transportable Array or PASSCAL deployments) may be applied to events that occurred earlier or later than the temporary network using permanent remote stations even when the temporary stations are not present.

In addition, the method has several evident limitations.

- It requires a relatively dense base network within an area of interest for at least a few months.
- It provides the best accuracy when the frequency derivative of the source phase is relatively small; for example, when the source mechanism is a vertical force or a center of compression, when the source depth is less than 1 km or more than 5 km, or when the source mechanism is nearly purely strike-slip, thrust, or normal.

The technique described here is the first attempt at such a nonstandard approach to locate regional events using ambient noise EGFs.

ACKNOWLEDGEMENTS

The facilities of the IRIS Data Management System, and specifically the IRIS Data Management Center, were used to access the waveforms and metadata required in this study. The IRIS DMS is funded by the National Science Foundation and specifically the GEO Directorate through the Instrumentation and Facilities Program of the National Science Foundation under Cooperative Agreement EAR-0552316. We are grateful to Drs. J. C. Pechmann and W. S. Arabasz (University of Utah) for their help in identifying well located events in Utah.

REFERENCES

- Barmin M.P., A.L. Levshin, Y. Yang, and M.H. Ritzwoller (2010), Epicentral location based on Rayleigh wave Empirical Green functions from ambient noise, submitted to *Geophys. J. Int.*
- Bensen, G.D., M.H. Ritzwoller, M.P. Barmin, A.L. Levshin, F. Lin, M.P. Moschetti, N.M. Shapiro, and Y. Yang (2007). Processing seismic ambient noise data to obtain reliable broad-band surface wave dispersion measurements, *Geophys. J. Int.*, 169(3), pp. 1239-1260, DOI:10.1111/j.1365-246X.2007.03374.x.
- Flinn, E.A. (1965). Confidence regions and error determinations for seismic event locations. *Rev. Geophys.*, 3, pp.157-185.
- Levshin, A.L., T.B. Yanovskaya, A.V. Lander, B.G. Bukchin, M.P. Barmin, L.I. Ratnikova, and E.N. Its (1989). *Seismic Surface Waves in Laterally Inhomogeneous Earth*, (V.I. Keilis-Borok, Ed.), Kluwer Academic Publishers. Dordrecht/Boston/London.
- Levshin, A.L., M.H. Ritzwoller, and J.S. Resovsky (1999). Source effects on surface wave group travel times and group velocity maps, *Phys. Earth Planet. Inter.*, 115, pp.293-312.
- Lin, F., M.P. Moschetti, and M.H. Ritzwoller (2008). Surface wave tomography of the western United States from ambient seismic noise: Rayleigh and Love wave phase velocity maps, *Geophys. J. Int.*, 173(1), pp. 281-298, doi:10.1111/j1365-246X.2008.03720.x.
- Moschetti, M.P., M.H. Ritzwoller, and N.M. Shapiro (2007). Surface wave tomography of the western United States from ambient seismic noise: Rayleigh wave group velocity maps, *Geochem., Geophys., Geosys.*, 8, Q08010, doi:10.1029/2007GC001655.
- Pechmann, J.C., W.I. Arabasz, K.L. Pankow, R. Burlacu, and M.K. McCarter (2007). Seismological report on the 6 Aug 2007 Crandall Canyon Mine Collapse in Utah, *Seismol. Res. Lett.*, 79, 5, pp. 620-636.
- Ritzwoller, M.H., M. P. Barmin, A.L. Levshin, and Y. Yang (2009). Epicentral location of regional seismic events based on empirical Green functions from ambient noise, in *Proceedings of the 31th Monitoring Research Review: Ground-Based Nuclear Explosion Monitoring Technologies*, LA-UR-09-05726, pp. 389-398.
- Shapiro, N.M. and M.H. Ritzwoller (2002). Monte-Carlo inversion for a global shear velocity model of the crust and upper mantle, *Geophys. J. Int.*, 151, pp. 88-105.

Table 1. UUSS and SLU event parameters for earthquakes in Utah.

event #	Date (y/m/d)	Time(h:m:s)	latitude	longitude	Depth (km)	mb	Error (km)	Error (s)
1	2007/08/18	13:16:13.46	38.070	-113.323	9.0*	3.65*	0.42	0.4
2	2007/11/05	21:48:00.61	39.346	-111.648	15.0*	3.76*	0.41	0.4
3	2008/02/01	21:36:54.23	41.809	-112.218	0.18	3.59	0.40	2.0
4	2008/02/01	3:26:01.41	41.690	-111.143	8.5	3.37	0.47	0.6

* Depth and magnitude are from SLU.

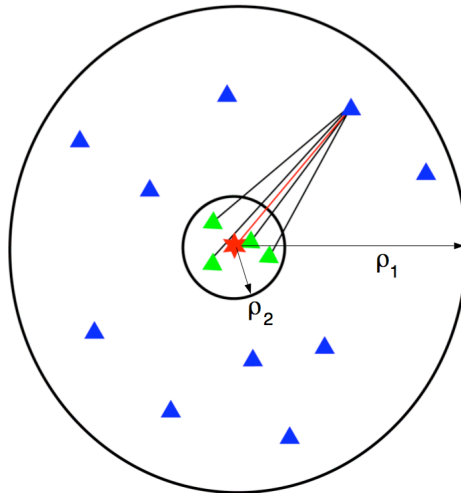


Figure 1. Schematic observational setting. A relatively dense set of temporary “base stations” (green triangles) encompasses the source region of interest (event is denoted by the red star). A sparse set of permanent “remote stations” (blue triangles) lies farther from the epicentral region.

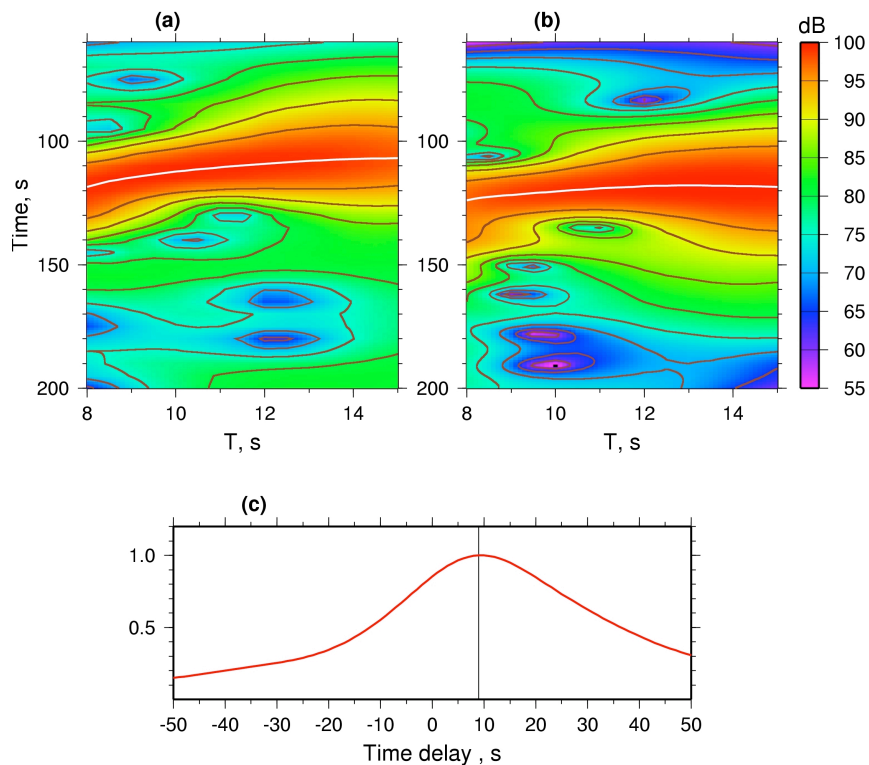


Figure 2. Illustration of location procedure based on cross-correlation of frequency-time (FT) representations of an event record and a Composite EGF. (a) FT-diagram of the event record for USArray Transportable Array station T14A following the Crandall Canyon Mine collapse (Pechmann et al., 2007) and the selected grid point. (b) FT-diagram of the Composite EGF for the same station and the same grid point. (c) Cross-correlogram of the two FT-representations in (a) and (b) showing a time delay of the maximum around 10 s.

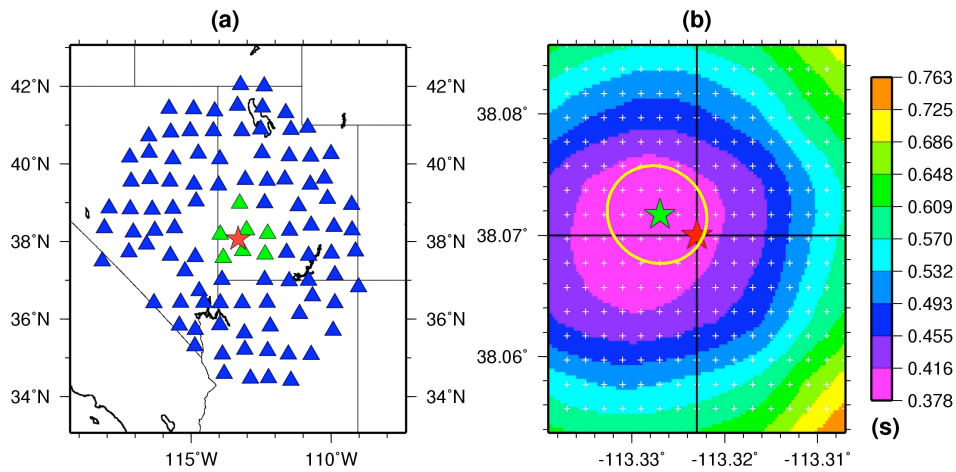


Figure 3. Location of event on 2007/08/18 (#1 in Table 1) in Utah. (a) Station configuration and misfit surface for the location (a) Symbols: base stations (green triangles), remote stations (blue triangles), and event location (red star). (b) Map of residuals: our event location (green star), UUSS location (red star), the 90% confidence ellipsoid (yellow line). Grid spacing of 200 m.

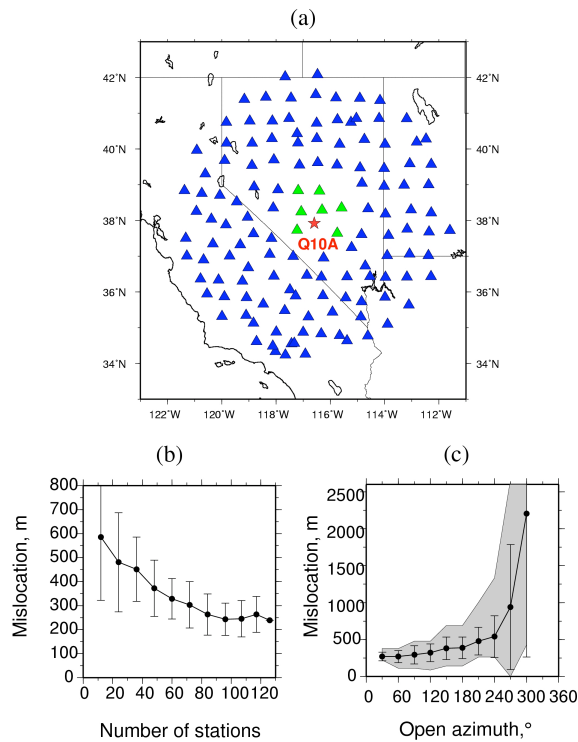


Figure 4. Location error as a function of the number of remote stations and azimuthal coverage. (a) Location of stations and virtual event (TA station Q10A): base stations (green triangles), remote stations (blue triangles), red star is the virtual source; (b) Effect of varying the number of remote stations on location accuracy; (c) Effect of the azimuthal coverage on location accuracy. Shaded domain covers all solutions for twelve realizations of each open azimuth. Error bars are 1 standard deviation.

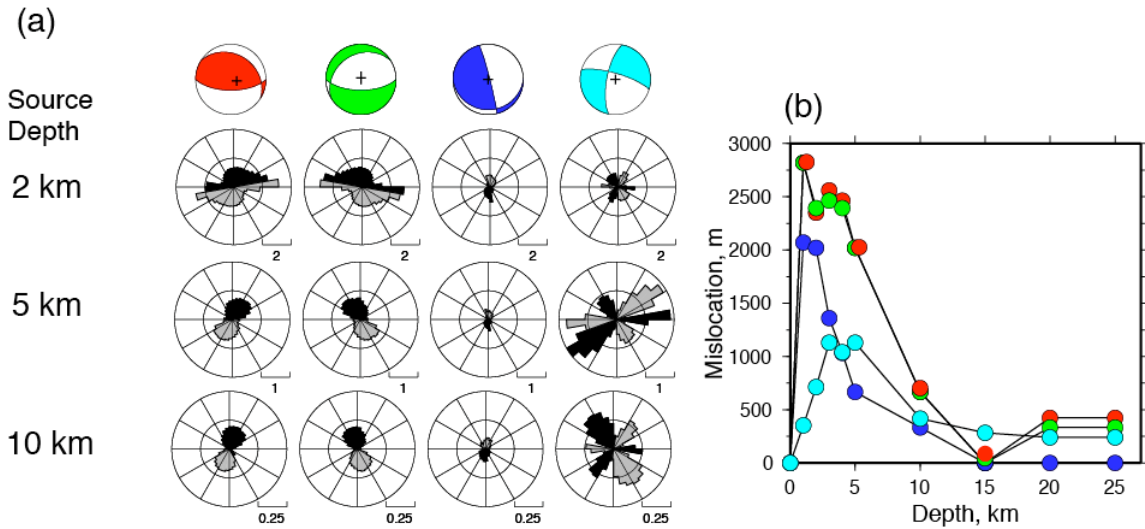


Figure 5. Simulation of the effect of source mechanism and depth on group time shifts and mislocation. Combination of base-remote stations used in the numerical simulation is shown in Figure 3a. (a) Source mechanisms (upper) and corresponding polar diagrams of group time residuals (lower) for the indicated source depths. Mechanism: red, near normal fault; green, near thrust fault; navy, near vertical thrust fault; light blue, near strike-slip fault. (b) Event mislocation for the four different source mechanisms as a function of depth. Symbol colors correspond to the source mechanisms shown in (a).

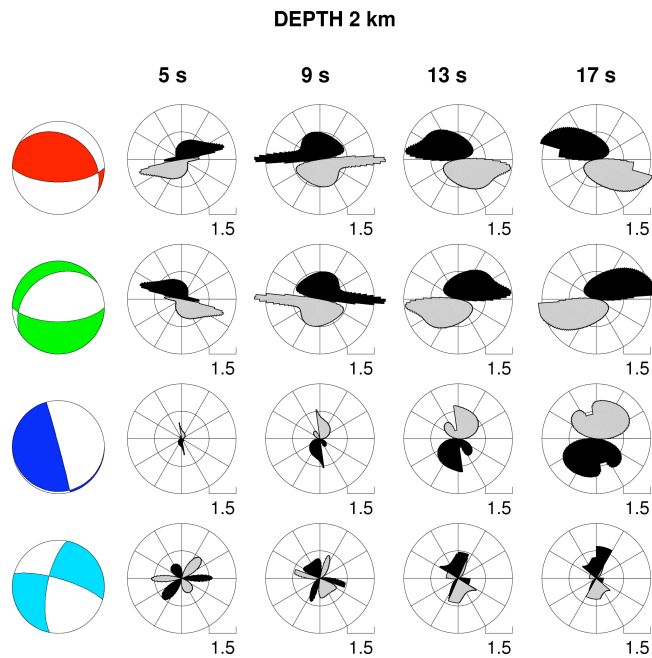


Figure 6. Theoretical prediction of group time delays at different periods for earthquakes at 2 km depth. Azimuthal dependence of group time delays are presented for four periods for four different source mechanisms (the same as in Fig. 5). The size of the time delays scale according to the bar at the lower right hand side of each component of the figure, in seconds.

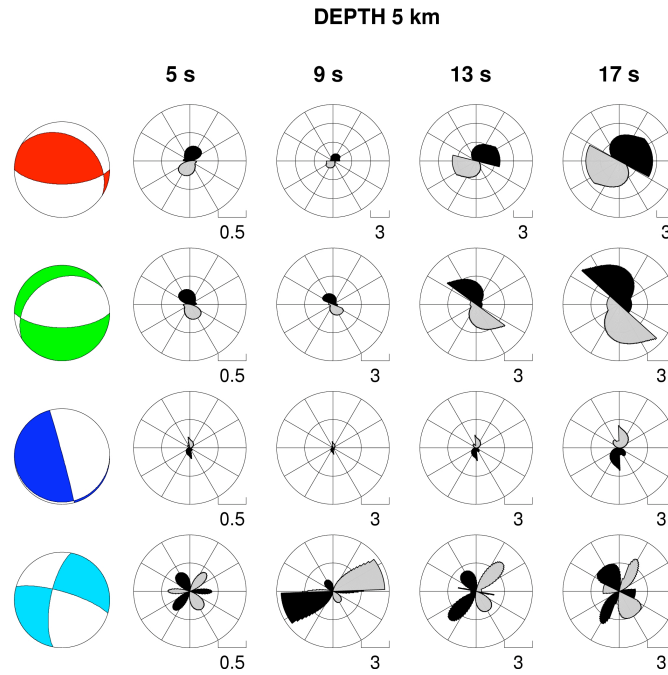


Figure 7. Theoretical prediction of group time delays at different periods. Same as Fig. 6, but for events at 5 km depth.

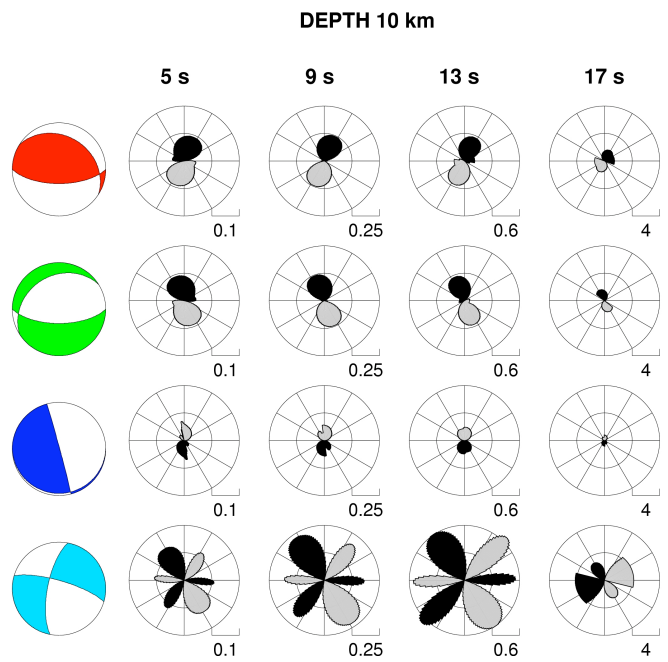


Figure 8. Theoretical prediction of group time delays at different periods. Same as Fig. 6, but for events at 10 km depth.